Available online at www.sciencedirect.com
ScienceDirect
Ceramics International 35 (2009) 409–413
CERAMICS INTERNATIONAL
www.elsevier.com/locate/ceramint

Cr_2O_3 doping in ZnO–0.5 mol% V_2O_5 varistor ceramics

H.H. Hng [*], P.L. Chan

School of Materials Science and Engineering, Division of Materials Science, Nanyang Technological University, Nanyang Ave, Singapore 639798, Singapore

Received 1 October 2007; received in revised form 30 October 2007; accepted 1 December 2007
Available online 8 April 2008

Abstract

The effects of the amount of Cr_2O_3 (0.5–4 mol%) on the microstructure and the electrical properties have been studied in a binary ZnO–0.5 mol% V_2O_5 system. The microstructure of the samples consists mainly of ZnO grains with $ZnCr_2O_4$ and α-$Zn_3(VO_4)_2$ as the minority secondary phases. The addition of Cr_2O_3 is found to be effective in controlling the abnormal ZnO grain growth often found in V_2O_5-doped ZnO ceramic system, and a more uniform microstructure can be obtained. The varistor performance is also improved as observed from the increase in the non-linear coefficient α of the Cr_2O_3-doped ZnO–V_2O_5 samples. The α value is found to increase with the amount of Cr_2O_3 for up to 3 mol% Cr_2O_3 content. Further increase in Cr_2O_3 is found to cause a decrease in the α value. The highest α value of 28.9 is obtained for the ZnO–0.5 mol% V_2O_5–3 mol% Cr_2O_3 sample.

Keywords: B. Microstructure-final; D. ZnO; E. Varistors

1. Introduction

Zinc oxide ceramics with the addition of small amounts of other metal oxides exhibit highly non-ohmic behaviour in current–voltage (*I*–*V*) characteristics, and are widely used as a voltage regulator and surge protector [1–3]. It is believed that this non-linear *I*–*V* characteristics arise from modifications to the electrical characteristics of the zinc oxide grain boundaries caused by the segregation of large ionic additives such as Bi [1–4], Pr [5,6], and Ba [7]. However, studies have shown that the light-metal oxide V_2O_5 is a potential varistor-forming ingredient for ZnO varistors [8–11]. The advantage of vanadium-doped ZnO varistor system is that the ceramics can be sintered at a relatively low temperature of about 900 °C, which allows the material to be cofired with a silver inner-electrode for applications in multilayer chip components. Moreover, V_2O_5 is a better sintering aid compared to Bi_2O_3 since it has been found that V_2O_5-doped ZnO materials can be densified to the same density at a lower temperature compared to Bi_2O_3-doped ZnO materials [11].

Transition metal oxides, such as MnO_2 and Cr_2O_3 additives are generally included to improve the non-ohmic properties of ceramics by increasing the surface-state density, through the formation of interstitial states and deep bulk traps [12]. They are considered as performance enhancers, in that they improve the non-linearity of the curve and enhance the energy absorption capability of ZnO varistor systems. Although there were numerous studies on the effects of various metal oxides on Bi_2O_3- and Pr_6O_{11}-doped ZnO varistors [13–16], such studies on the performance of ZnO–V_2O_5 varistor systems are limited. Hence, the purpose of this study is to ascertain whether Cr_2O_3 beneficially affect the ZnO–V_2O_5 system, just as they do for the ZnO–Bi_2O_3 varistor system. The effects of Cr_2O_3 content on the microstructure and the electrical characteristics in a binary ZnO–0.5 mol% V_2O_5 system were studied. X-ray powder diffraction (XRPD), scanning electron microscopy (SEM), transmission electron microscopy (TEM) and standard electrical measurement procedures were used.

2. Experimental procedures

2.1. Sample preparation

High purity oxide powder starting materials were used for the preparation of the ZnO varistor samples. The powders were obtained from Sigma–Aldrich of purity as indicated in wt.%: ZnO (99.9%), V_2O_5 (99.6%) and Cr_2O_3 (99.9%). Cr_2O_3, in the

---

[*] Corresponding author. Tel.: +65 67904140; fax: +65 67909081.
E-mail address: ashhhng@ntu.edu.sg (H.H. Hng).

0272-8842/$34.00 © 2008 Elsevier Ltd and Techna Group S.r.l. All rights reserved.
doi:10.1016/j.ceramint.2007.12.004

range of 0–4 mol%, was mixed with a mixture of ZnO–0.5 mol% V_2O_5 powder by ball milling with alumina balls and deionised water for 24 h. The mixtures were then dried, pressed into pellets, and sintered in an atmosphere of ambient air for 4 h at 900 °C and cooled at 5 °C/min.

2.2. Characterisation

For electrical measurements, the as-sintered specimens were lapped on both surfaces to ensure flat and parallel surfaces. They were coated with conductive silver paint on both surfaces, then heat cured to provide ohmic contacts. The current–voltage (*I–V*) characteristics were determined at room temperature using a variable dc power supply (Kikusui Withstanding Voltage Tester, TOS 5051). X-ray analysis of the sintered samples was carried out using Cu Kα radiation on a Shimadzu Lab X-ray diffractometer. Microstructures were examined by SEM (JEOL JSM 5310) equipped with energy dispersive X-ray (EDX) analysis. Specimens for TEM were prepared using standard ion beam thinning methods and examined using a JEOL 2010 at 200 kV.

3. Results and discussion

3.1. X-ray powder diffraction

For all the samples, other than the major ZnO phase, $ZnCr_2O_4$ and α-$Zn_3(VO_4)_2$ were detected as minor secondary phases. A typical XRPD trace is shown in Fig. 1. The formation of the $ZnCr_2O_4$ spinel phase (JCPDS 22-1107) is often reported in Bi_2O_3-doped ZnO varistor systems containing Cr_2O_3 [14–16]. This occurs when the amount of added Cr_2O_3 is much higher than the amount of Sb_2O_3 (if present) and when the solubility of Cr_2O_3 in Bi_2O_3 is exceeded. The occurrence of the $Zn_3(VO_4)_2$ phase is also common for all reported ZnO–V_2O_5 system [8–11]. It was proposed that the V_2O_5 additives can enhance the densification and grain growth behaviour of the ZnO–V_2O_5 materials due to the formation of $Zn_3(VO_4)_2$, which acts as a liquid-phase sintering aid at high temperature [8]. It was earlier reported that different types of $Zn_3(VO_4)_2$ polymorphs were formed in the V_2O_5-doped ZnO varistors, and the polymorph types are dependent on the type of additives oxides introduced into the system, as well as on the V_2O_5 content [9]. Later studies [17,18] have queried the existence of polymorphism in $Zn_3(VO_4)_2$, and it was confirmed that neither β- nor γ-$Zn_3(VO_4)_2$ phases exist. In fact, it was deduced that the β-phase is the $Zn_4V_2O_9$ phase, and the γ-phase may be another oxide compound composing of zinc, vanadium and manganese or a mixture of compounds. In the current study for the specimens containing Cr_2O_3, only the α-$Zn_3(VO_4)_2$ phase (JCPDS 34-378) was identified.

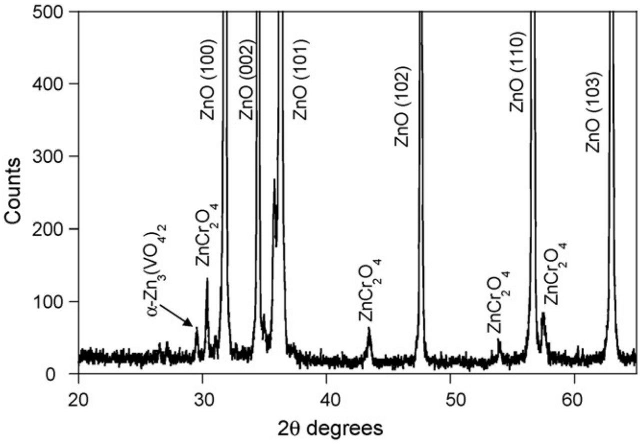

Fig. 1. A typical XRPD trace (Cu Kα) for a ZnO–V_2O_5–Cr_2O_3 sample.

3.2. Microstructural observations

In general, the microstructural observations are consistent with the reported liquid-phase sintering mechanism for ZnO varistors containing V_2O_5. ZnO has a eutectic reaction with $Zn_3(VO_4)_2$ at ~890 °C [19], and for sintering at ≥900 °C, the liquid phase of $Zn_3(VO_4)_2$ will enhance densification by solution and reprecipitation of ZnO. In all our specimens, the microstructure consisted of ZnO grains surrounded by a V-rich phase of $Zn_3(VO_4)_2$, indicative of liquid-phase sintering. TEM observation (Fig. 2) revealed the existence of the minor secondary phases localized at the grain boundaries or distributed in the ZnO grains. The distributions of the α-$Zn_3(VO_4)_2$ and $ZnCr_2O_4$ phases along the grain boundaries could be observed. The α-$Zn_3(VO_4)_2$ phase was found to be embedded at the triple or multiple grain junctions, and the observation is consistent with our previous studies [9]. The $ZnCr_2O_4$ grains were found scattered along the grain boundaries. This is consistent with the observations reported by Kim et al. [14] in their Cr_2O_3-doped ZnO–Bi_2O_3 varistor system, where $ZnCr_2O_4$ grains of ~1 μm in size were found as aggregates located at the grain boundaries.

Low magnification SEM images (Fig. 3) were obtained to determine the average ZnO grain size of V_2O_5-doped ZnO varistors. The average ZnO grain sizes shown in Table 1 were

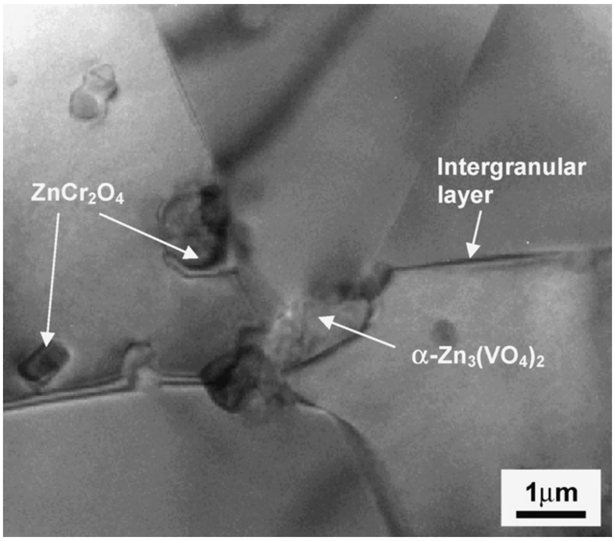

Fig. 2. TEM micrograph of ZnO–0.5 mol% V_2O_5–2 mol% Cr_2O_3 (ZVCr2) sample showing the secondary minor phases.

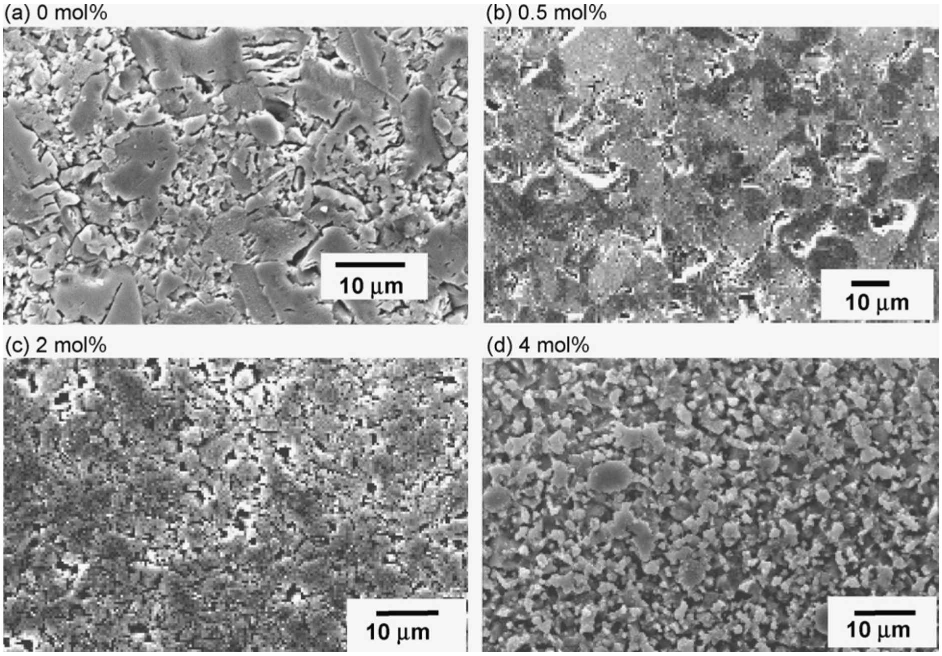

Fig. 3. SEM micrographs of V_2O_5-doped ZnO varistors containing various amounts of Cr_2O_3.

obtained from the SEM micrographs by multiplying the average linear intercept length of the grains by 1.56 [20]. The binary system (ZV) showed exaggerated ZnO grain growth which previous studies have also reported [8–11]. It is also noted that every exaggerated grain contains a (0 0 0 1) inversion boundary (IB), which is the cause of the exaggerated grain growth in ZnO ceramics [21,22]. The microstructure consists of a few large grains (~10 μm) surrounded with numerous smaller grains (~1 μm). Hence, it should be noted that the average grain size of 6.9 μm may not be an accurate representative of the actual grain size for sample ZV.

With the addition of Cr_2O_3 to the ZnO–0.5 mol% V_2O_5 ceramic system, microstructures of more equiaxed and homogeneous ZnO grains were obtained. The initial addition of 0.5 mol% Cr_2O_3 saw an increase in the ZnO grain size. Subsequent increase in Cr_2O_3 content up to 4 mol% saw a gradual decrease in the average ZnO grain size. The results suggest that the addition of Cr_2O_3 has a beneficial effect in suppressing the exaggerated ZnO grain growth that is often observed in ZnO–V_2O_5 systems, and it is an effective grain growth inhibitor. Addition of Cr_2O_3 as a grain size inhibitor has also been reported in studies on ZnO–Bi_2O_3 varistor systems [13–16]. The grain size reduction was suggested to be attributed to the contiguity of the grains. The degree of contact, or the contiguity, of ZnO grains for specimens containing Cr was observed to be larger than those without Cr. This suggests that there is lower wettability of the liquid phase during sintering for the Cr-containing specimens. Therefore, it is believed that the addition of the Cr changed the nature of the liquid phase during sintering, which lowered the wettability, resulting in reduced grain growth and control the abnormal ZnO grain growth in ZnO–V_2O_5 systems. In addition, the presence of the secondary minor phases ($Zn_3(VO_4)_2$ and $ZnCr_2O_4$) at the grain boundaries may also play a role in controlling the ZnO grain growth in this ceramic system.

3.3. Current–voltage characteristics

The effects of Cr_2O_3 addition on the electrical properties of the V_2O_5-based ZnO materials were characterised by their electric field–current density (*E–J*) properties. Typical *E–J*

Table 1
Summary of sample composition, average ZnO grain size and electrical results for the different ZnO–V_2O_5–Cr_2O_3 varistor ceramics

Sample	Composition	Average ZnO grain size (μm)	$E_{1\,mA/cm^2}$ (V/cm)[a]	J_{leak} ($\times 10^{-4}$ A/cm^2)[b]	Non-linear coefficient, α[c]
ZV	ZnO–0.5 mol% V_2O_5	6.9	80	7	10.3
ZVCr0.5	ZnO–0.5 mol% V_2O_5–0.5 mol% Cr_2O_3	20.2	100	7	12.7
ZVCr1	ZnO–0.5 mol% V_2O_5–1 mol% Cr_2O_3	18.3	200	5	13.4
ZVCr2	ZnO–0.5 mol% V_2O_5–2 mol% Cr_2O_3	6.7	1200	4.8	27.2
ZVCr3	ZnO–0.5 mol% V_2O_5–3 mol% Cr_2O_3	5.5	1800	4	28.9
ZVCr4	ZnO–0.5 mol% V_2O_5–4 mol% Cr_2O_3	5.0	2000	4	17.2

[a] Electric field at 1 mA/cm^2.

[b] Current density at $0.8E_{1\,mA/cm^2}$.

[c] $\alpha = \log(J_2/J_1)/\log(E_2/E_1)$ where $J_1 = 10$ mA/cm^2 and $J_2 = 100$ mA/cm^2.

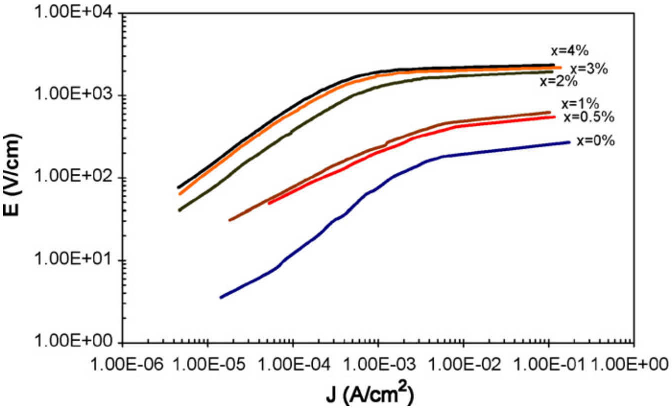

Fig. 4. The electric field–current density (*E*–*J*) curves for the various ZnO–V_2O_5–Cr_2O_3 samples.

curves are shown in Fig. 4. The corresponding parameters obtained from these curves are summarised in Table 1, where the point at which non-linearity begins is given by the onset electric field $E_{1\,\mathrm{mA/cm^2}}$ and leakage current density J_{leak}.

The effects of Cr_2O_3 content on the various electrical parameters are presented graphically in Fig. 5. The leakage current density J_{leak} is not affected much by the addition of Cr_2O_3. However, the onset electric field $E_{1\,\mathrm{mA/cm^2}}$ and the non-linear coefficient α are greatly affected by the Cr_2O_3 content.

$E_{1\,\mathrm{mA/cm^2}}$ increases as the amount of Cr_2O_3 is increased. The increase in the breakdown electric field as Cr_2O_3 increased is mainly attributed to the decrease in the grain size, which give rise to an increase in grain boundaries. Kim et al. [14] also observed similar trend in their study of the effects of Cr_2O_3 in a multi-component ZnO–Bi_2O_3 varistor material.

The non-linear coefficient α, on the other hand, exhibits a different trend. The α value increases steadily as Cr_2O_3 content increases up to 3 mol%. When Cr_2O_3 content was further increased to 4 mol%, the α value decreased. Such improvement in the α value with the addition of Cr_2O_3 has also been reported in ZnO–Bi_2O_3 multi-component varistor system [13]. It has been postulated that transition metal oxides, such as Cr, Co and Mn, are involved in the formation of interfacial states and deep bulk traps at grain boundaries [23], providing large potential barriers to give better non-linear characteristics [24].

It is noted that the improvement was only for up to 0.1 mol% Cr_2O_3 in the ZnO–Bi_2O_3–Sb_2O_3 multi-component varistor system [13]. Further increase in Cr_2O_3 concentration was found to have a deleterious effect on the potential barrier at the grain boundary, which increases the leakage current and decreases the α value in the ZnO–Bi_2O_3 multi-component varistor system. Excess Cr^{3+} ions, not dissolved by the spinel ($Zn_7Sb_2O_{12}$) or Bi-rich phases, were assumed to have segregated at grain boundaries to cause a decrease in the grain-boundary electrical resistance. In the current study for the ZnO–V_2O_5 varistor system, the optimum Cr_2O_3 content is much higher at 3 mol%. A possible reason may be more Cr^{3+} ions can be dissolved in the V-rich phases rather than the Bi-rich phases. Furthermore, most of the Cr added into the ZnO–V_2O_5 system would have been used to form the $ZnCr_2O_4$ phase. As compared, in the ZnO–Bi_2O_3–Sb_2O_3 multi-component varistor system, the $ZnCr_2O_4$ phase was not formed due to the addition of Sb_2O_3, in which case, the spinel $Zn_7Sb_2O_{12}$ phase was formed instead.

Lastly, another factor that may affect the varistor behaviour is the presence of the minor secondary phases in the ZnO–V_2O_5 system. In a previous study, experimental results suggested that the secondary phase $Zn_3(VO_4)_2$ plays a role in the electrical performance of ZnO–V_2O_5 varistor [9]. It was found that it is desirable to have γ-phase rather than the α- or β-phase as a secondary phase. (*Although it was mentioned earlier that there is*

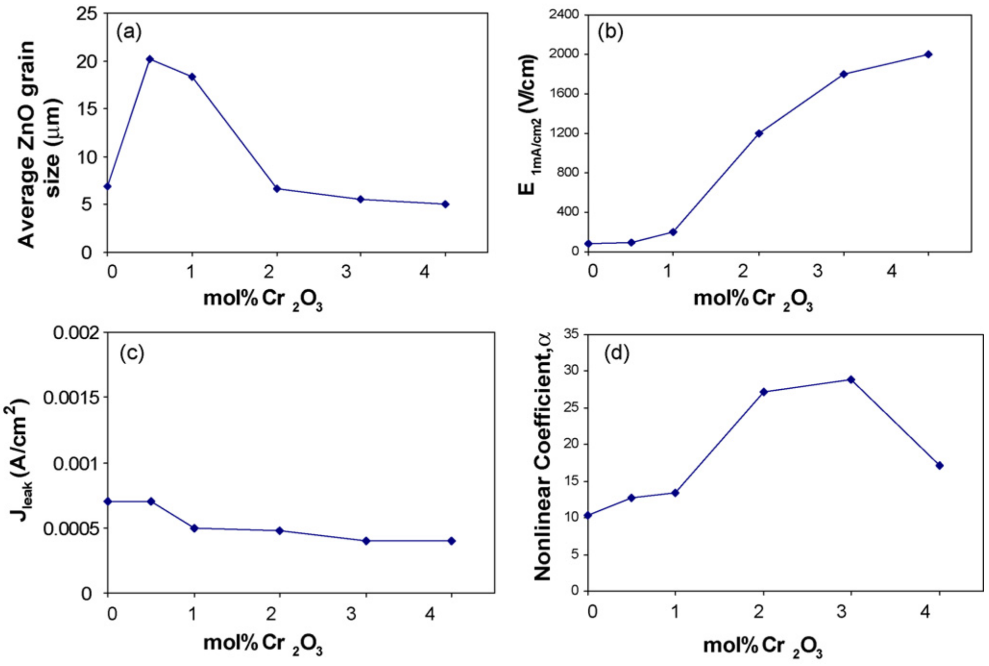

Fig. 5. Effects of Cr_2O_3 content on (a) average ZnO grain size; (b) onset electric field, $E_{1\,\mathrm{mA/cm^2}}$; (c) leakage current density, J_{leak}; and (d) non-linear coefficient, α.

no polymorphism in $Zn_3(VO_4)_2$, *for comparison purposes, we will conform to these notations to avoid confusion.*) Thus, it can also be inferred that the α-$Zn_3(VO_4)_2$ phase detected for our current specimens is not as beneficial, and hence the improvement in the varistor behaviour in the current study for the addition of Cr_2O_3 is less as compared to the addition of MnO_2 in our previous study [10], where the γ-phase was formed instead.

4. Conclusions

Addition of Cr_2O_3 to the binary ZnO–0.5 mol% V_2O_5 system controlled the abnormal ZnO grain growth and produced a more uniform microstructure. The microstructure of the samples consists mainly of ZnO grains with $ZnCr_2O_4$ and α-$Zn_3(VO_4)_2$ as the minority secondary phases. The non-linear coefficient α increases as the amount of Cr_2O_3 additive is increased up to 3 mol%. Further increase in Cr_2O_3 content caused a decrease in the α value. A highest non-linear coefficient of 28.9 was obtained for the sample containing 3 mol% Cr_2O_3 in 0.5 mol% V_2O_5-doped ZnO varistor.

References

[1] K. Eda, A. Iga, M. Matsuoka, Degradation mechanism of non-ohmic zinc oxide ceramics, J. Appl. Phys. 51 (1980) 2678–2684.

[2] L.M. Levinson, H.R. Philipp, Zinc oxide varistors—a review, Am. Ceram. Soc. Bull. 65 (1986) 639–646.

[3] T.K. Gupta, Application of zinc oxide varistors, J. Am. Ceram. Soc. 73 (1990) 1817–1840.

[4] J. Wong, Sintering and varistor characteristics of ZnO–Bi_2O_3 ceramics, J. Appl. Phys. 51 (1980) 4453–4459.

[5] A.B. Alles, R. Puskas, G. Callahan, V.L. Burdick, Compositional effects on the liquid-phase sintering of praseodymium oxide-based zinc oxide varistors, J. Am. Ceram. Soc. 76 (1993) 2098–2102.

[6] H.H. Hng, K.M. Knowles, Microstructure and current–voltage characteristics of praseodymium-doped zinc oxide varistors containing MnO_2, Sb_2O_3 and Co_3O_4, J. Mater. Sci. 37 (2002) 1143–1154.

[7] M. Matsuoka, T. Masuyama, Y. Lida, Voltage non-linearity of zinc oxide ceramics doped with alkali earth metal oxide, Jpn. J. Appl. Phys. 8 (1969) 1275–1276.

[8] J.K. Tsai, T.B. Wu, Microstructure and nonohmic properties of binary ZnO–V_2O_5 ceramics sintered at 900 °C, Mater. Lett. 26 (1996) 199–203.

[9] H.H. Hng, K.M. Knowles, Microstructure and current–voltage characteristics of multicomponent vanadium-doped zinc oxide varistors, J. Am. Ceram. Soc. 83 (2000) 2455–2462.

[10] H.H. Hng, P.L. Chan, Effects of MnO_2 doping in V_2O_5-doped ZnO varistor system, Mater. Chem. Phys. 75 (2002) 61–66.

[11] C.S. Chen, C.T. Kuo, T.B. Wu, I.N. Lin, Microstructure and electrical properties of V_2O_5-based multicomponent ZnO varistors prepared by microwave sintering process, Jpn. J. Appl. Phys., Part 1 36 (1997) 1169–1175.

[12] F. Greuter, G. Blatter, M. Rossinelli, F. Stucki, Conduction Mechanism in ZnO-varistors: an Overview, in: Proceedings of the 2nd International Varistors Conference, 1988, p. 31.

[13] S.A. Pianaro, E.C. Pereira, L.E. Bulhões, J.A. Varela, Effects of Cr_2O_3 on the electrical properties of multicomponent ZnO varistors at the pre-breakdown region, J. Mater. Sci. 30 (1995) 133–141.

[14] Y.H. Kim, H. Kawamura, M. Nawata, The effect of Cr_2O_3 additive on the electrical properties of ZnO varistor, J. Mater. Sci. 32 (1997) 1665–1670.

[15] S.G. Cho, H. Lee, H.S. Kim, Effect of chromium on the phase evolution and microstructure of ZnO doped with bismuth and antimony, J. Mater. Sci. 32 (1997) 4283–4287.

[16] Y. Shimizu, F.C. Lin, Y. Takao, M. Egashira, Zinc oxide varistor gas sensors: effect of chromium (III) oxide and yttrium oxide additives on the hydrogen-sensing properties, J. Am. Soc. 81 (1998) 1633–1643.

[17] H.H. Hng, K.M. Knowles, P.A. Midgley, Zinc vanadates in vanadium oxide-doped zinc oxide varistors, J. Am. Ceram. Soc. 84 (2001) 435–441.

[18] M. Kurzawa, I. Rychlowska-Himmel, M. Bosacka, A. Blonska-Tabero, Reinvestigation of phase equilibria in the V_2O_5–ZnO system, J. Therm. Anal. Calorim. 64 (2001) 1113–1119.

[19] J.J. Brown, F.A. Hummel, Reactions between ZnO and selected oxides of elements of groups IV and V, Trans. Br. Ceram. Soc. 64 (1965) 419–437.

[20] M.I. Mendelson, Average grain size in polycrystalline ceramics, J. Am. Ceram. Soc. 52 (1969) 443–446.

[21] N. Daneu, A. Recnik, S. Bernik, Grain growth control in Sb_2O_3-doped zinc oxide, J. Am. Ceram. Soc. 86 (2003) 1379–1384.

[22] S. Bernik, N. Daneu, A. Recnik, Inversion boundary induced grain growth in TiO_2 or Sb_2O_3 doped ZnO-based varistor ceramics, J. Eur. Ceram. Soc. 24 (2004) 3703–3708.

[23] K. Eda, Zinc oxide varistors, IEEE Electric. Insul. Mag. 5 (1989) 28–41.

[24] S. Ezhilvalavan, T.R.N. Kutty, Dependence of non-linearity coefficients on transition metal oxide concentration in simplified compositions of ZnO + Bi_2O_3 + MO varistor ceramics (M=Co or Mn), J. Mater. Sci.: Mater. Electron. 7 (1996) 137–148.